Title: A possible Middle Pleistocene Denisovan from the Annamite Chain of northern Laos

Authors: Fabrice Demeter[#*1,2], Clément Zanolli[#*3], Kira E. Westaway[4], Renaud Joannes-Boyau[5,6], Philippe Duringer[7], Mike W. Morley[8], Frido Welker[9], Patrick L. Rüther[10], Matthew M. Skinner[11,12], Hugh McColl[1], Charleen Gaunitz[1], Lasse Vinner[1], Tyler E. Dunn[13], Jesper V. Olsen[10], Martin Sikora[1], Jean-Luc Ponche[14], Eric Suzzoni[15], Sébastien Frangeul[15], Quentin Boesch[7], Pierre-Olivier Antoine[16], Lei Pan[17, 18], Song Xing[17,19], Jian-Xin Zhao[20], Richard M. Bailey[21], Souliphane Boualaphane[22], Phonephanh Sichanthongtip[22], Daovee Sihanam[22], Elise Patole-Edoumba[23], Françoise Aubaile[2], Françoise Crozier[24], Nicolas Bourgon[12], Alexandra Zachwieja[25], Thonglith Luangkhoth[22], Viengkeo Souksavatdy[22], Thongsa Sayavongkhamdy[22], Enrico Cappellini[9], Anne-Marie Bacon[26], Jean-Jacques Hublin[12, 27], Eske Willerslev[1,28,29,30], Laura Shackelford[#*31, 32]

[#]These authors contributed equally to this work
[*]Corresponding authors

Affiliations:
[1] Lundbeck Foundation GeoGenetics Centre, Globe Institute, University of Copenhagen, Copenhagen, Denmark.
[2] Eco-anthropologie (EA), Muséum national d'Histoire naturelle, CNRS, Université de Paris, Musée de l'Homme 17 place du Trocadéro 75016 Paris, France.
[3] Univ. Bordeaux, CNRS, MCC, PACEA, UMR 5199, 33600 Pessac, France.
[4] 'Traps' Luminescence Dating Facility, Department of Earth and Environmental Sciences, Macquarie University, Sydney, Australia.
[5] GARG, Southern Cross GeoScience, Southern Cross University, NSW, Australia.
[6] Centre for Anthropological Research, University of Johannesburg, Gauteng Province, South Africa.
[7] Ecole et Observatoire des Sciences de la Terre, Institut de Physique du Globe de Strasbourg (IPGS), UMR 7516 CNRS, Université de Strasbourg, France.
[8] Archaeology, College of Humanities and Social Sciences, Flinders University, Sturt Road, Bedford Park, Adelaide, Australia.
[9] Section for Evolutionary Genomics, Globe Institute, University of Copenhagen, Denmark.
[10] The Novo Nordisk Foundation Center for Protein Research, University of Copenhagen, Copenhagen, Denmark.
[11] School of Anthropology and Conservation, University of Kent, United Kingdom.
[12] Department of Human Evolution, Max Planck Institute for Evolutionary Anthropology, Leipzig, Germany.
[13] Department of Medical Education, Creighton University School of Medicine, USA.
[14] Université de Strasbourg, Laboratoire Image, Ville Environnement, UMR 7362 UdS CNRS, France.
[15] Spitteurs Pan, technical cave supervision and exploration, La Chapelle en Vercors, France.
[16] Institut des Sciences de l'Évolution, Univ Montpellier, CNRS, IRD, Montpellier, France.
[17] Key Laboratory of Vertebrate Evolution and Human Origins, Institute of Vertebrate Paleontology and Paleoanthropology, CAS, Beijing, China.
[18] State Key Laboratory of Palaeobiology and Stratigraphy, Nanjing Institute of Geology and Palaeontology, CAS, Nanjing, China.

[19] CAS Center for Excellence in Life and Paleoenvironment, Beijing, China.
[20] School of Earth and Environmental Sciences, University of Queensland, Brisbane, Queensland, Australia.
[21] School of Geography and the Environment, University of Oxford, Oxford, United Kingdom.
[22] Ministry of Information, Culture and Tourism, Laos PDR.
[23] Museum d'histoire naturelle de La Rochelle, France.
[24] IRD, DIADE, Montpellier, France.
[25] Department of Biomedical Sciences, University of Minnesota Medical School Duluth, USA.
[26] Université de Paris, BABEL CNRS UMR 8045, France.
[27] Collège de France, Paris, France.
[28] Department of Zoology, University of Cambridge, United Kingdom.
[29] Wellcome Trust Sanger Institute, Cambridge, United Kingdom.
[30] Danish Institute for Advanced Study, University of Southern Denmark, Copenhagen, Denmark.
[31] Department of Anthropology, University of Illinois at Urbana-Champaign, Urbana, IL, USA.
[32] Carle Illinois College of Medicine, University of Illinois at Urbana-Champaign, Urbana, IL, USA.

Abstract: The Pleistocene presence of the genus *Homo* in continental Southeast Asia is primarily evidenced by a sparse stone tool record and rare human remains. Here we report the first Middle Pleistocene hominin specimen from Laos, with the discovery of a molar from the Tam Ngu Hao 2 (Cobra Cave) limestone cave in the Annamite Mountains. The age of the fossil-bearing breccia ranges between 164-131 kyr, based on the Bayesian modelling of luminescence dating of the sedimentary matrix from which it was recovered, U-series dating of an overlying flowstone, and U-series–ESR dating of associated faunal teeth. Analyses of the internal structure of the molar in tandem with palaeoproteomic analyses of the enamel indicate that the tooth derives from a young, likely female, *Homo* individual. The close morphological affinities with the Xiahe specimen from China indicate that they belong to the same taxon and that Tam Ngu Hao 2 represents, most likely, a Denisovan.

MAIN TEXT

Introduction: From the Early to Late Pleistocene, the presence of *Homo erectus* is well documented in Asia, notably in China and Indonesia [1–3]. However, the taxonomic attribution of most Asian late Middle Pleistocene *Homo* specimens remains a matter of contention [4-7]. The recent description and analysis of the Harbin cranium from China has reignited this debate by suggesting its attribution to a new species named *Homo longi* [8], but this taxonomic attribution of this specimens remains highly debated. In fact, the Harbin cranium shows close morphological similarities with other late Middle to early Late Pleistocene Asian *Homo* specimens from Dali, Xujiayao, Xuchang and Hualongdong, whose taxonomy remains unclear [4,9,10]. These fossils are considered to belong to a different taxon than *H. erectus* and are often grouped under the generic label 'archaic humans' [9,10]. Due to the combination of features they exhibit, including Neanderthal-like traits, it has been suggested that they belong to an Asian sister taxon of Neanderthals, the Denisovans, even if this attribution to the latter group remains under debate [5.11.12]. The small number of fossils currently securely attributed to this group (Denisova 2, a lower left molar; Denisova 3, a distal manual phalanx; Denisova 4, an upper left M3; Denisova 8, an upper molar; and the Xiahe mandible) [13–16] prohibits a clear morphological picture of the overall Denisovan morphology. Their geographic distribution also remains debated. Modern Papuans, Aboriginal Australians, Oceanic/Melanesian, Philippine Ayta groups and, to a much lesser extent, mainland Southeast Asian populations, retain a Denisovan genetic legacy [14,17,18,19]. Combined paleoproteomic and morphometric analyses recently suggested that the Middle Pleistocene Xiahe mandible from Baishiya Karst Cave belonged to a Denisovan, extending the known range of this group onto the Tibetan Plateau [15]. However, there is still no fossil evidence explaining the Denisovans genetic imprint on modern southeast Asian populations and—due to the paucity of the Middle Pleistocene fossil record—it is still unknown whether one or more human lineages (co)existed in continental southern Asia. We present here the first unambiguous Middle Pleistocene *Homo* specimen from mainland southeast Asia and discuss its taxonomic attribution and implications for human evolution in the region.

In December 2018, a hominin permanent lower molar was recovered from a breccia block at Tam Ngu Hao 2 (Cobra Cave), Huà Pan province, Laos (20°12'41.5"N, 103°24'32.2"E, altitude 1,116 m; Fig. 1, Fig. S1). The tower karst in which the cave was formed is positioned on the south-eastern side of P'ou Loi Mountain with an entrance located 34 m above the alluvial plain (Fig. 1A, Fig. S1). The site was discovered during a survey of the area around Tam Pà Ling,

where early *Homo sapiens* fossils have previously been recovered [20-22]. The tooth (TNH2-1) is a mandibular left permanent molar crown germ (Fig. 2A-F; Fig. S2), and the absence of occlusal and interproximal wear combined with the incipient root formation suggests that the tooth was unerupted at the time of the individual's death. The morphology of the tooth is compatible with an attribution to either a first or a second lower molar (Supplementary Material). In either case, considering the early maturational stage of the root, this tooth belonged to a juvenile individual corresponding to an age ranging from 3.5 to 8.5 years following modern developmental standards [23].

To best document THN2-1, morphological description and comparative analyses were performed. We also developed a specific sampling protocol that allowed us to sample for palaeoproteomic and future isotopic analyses while preserving the whole occlusal surface morphology of the crown. Sampling for these destructive analyses took place after microCT analyses of the entire tooth, ensuring full morphological data were saved. No additional sampling for ancient DNA analyses was performed at this stage given the old age of the specimen and the tropical conditions under which the sediment and fossils were deposited. The invasive sampling strategy to collect dental tissues for molecular analyses only focused on the distal part of the inferior aspect of the crown, keeping the mesial portion of the crown intact.

Results

Context and Dating

The geological setting, stratigraphy and micromorphology of the sediment sequence were analysed to obtain a comprehensive, multi-scalar assessment of the depositional context and taphonomic history of the fossils recovered from the cave (Supplementary Material). The partially eroded sediments that infill the studied entrance passage comprise a lower and an upper facies representing two phases of sediment accumulation separated by an erosional surface and an unknown period of time (Fig. 1B). The lower facies (Lithological Unit 1, LU1) is weakly cemented and forms an arenitic silty clay deposit that is devoid of fossils (Fig. 1E). The upper, fossiliferous facies (Lithological Unit 2, LU2) is well cemented and coarse grained, containing intrakarstic angular limestone clasts and extrakarstic rounded pebbles, forming a very hard breccia/conglomerate layer from which skeletal elements—and in particular, teeth—were recovered in high frequencies (Fig. 1D). The change in lithology between the two facies most

likely reflects a reconfiguration of the karstic hydrological system as would be associated with a major flood, eroding space in LU1 onto which the sediments of LU2 were unconformably overlain. The sediments of LU2 are laterally contiguous and densely packed throughout the exposure excavated for this study, precluding major reworking of material and confirming the stratigraphic context of the fossils contained within, including the hominin tooth (see detailed observations described in Supplementary Material). The upper facies (LU2) is draped with two carbonate flowstones, indicating a final change in hydrology and the passage of surface water out of the cave and the precipitation of laminar speleothem (Fig. 1C).

Three bovid teeth (TNH2-10/CC10, TNH2-11/CC11, TNH2-12/CC12) recovered from the upper fossil-bearing breccia (LU2) were directly dated using coupled uranium series and electron spin resonance (US-ESR), providing a weighted mean age estimate of 151+/-37 thousand years ago (kyr) (2-sigma) (Fig. 1B; Tables S1, S2) and an age range of 188-117 kyr. Two large blocks of breccia (LCC1 and LCC2) from LU2 (upper) and one block of the silty clay unit (LCC3) from LU1 (lower) were removed for luminescence dating (Fig. 1B). These samples produced coeval age estimates of 143 ± 24 kyr (LCC1) and 133 ± 19 kyr (LCC2) for the deposition of the LU2 breccia and 248 ± 31 kyr (LCC3) for the underlying LU1 silty clay deposit (Table S3). These ages are in stratigraphic agreement with the age of the overlying flowstone (CCF1), which was precipitated earlier than 104 ± 27 kyr based on the weighted mean of U-series age estimates on four separate sub-samples of flowstone carbonate (Table S4). Bayesian modelling was performed on all independent age estimates to determine an overall geochronological framework for the site and tooth (Supplementary Material and Fig. S3). The fossiliferous breccia including the tooth was deposited between 164-131 kyr (at 68% confidence limit).

Fauna

The Tam Ngu Hao 2 faunal assemblage comprises 186 identified dentognathic specimens (NISP) dominated by isolated teeth of large mammals, including several megaherbivores (Table S5). Their analyses reveal typical taphonomic pathways of assemblages from karstic systems in terms of representation of specimens and types of damage. Due to the energy associated with the deposition of (LU2), only teeth of large mammals are present in the assemblage, and we note the absence of small and light teeth of any microvertebrates. Moreover, most teeth are gnawed by porcupines, known to be a major accumulator agent in the region [24]. Therefore, the poor

preservation of specimens as shown in Fig. S15, precludes identification to the species level for most of the recorded taxa. The fauna bears close affinities to those known from the late Middle Pleistocene of southern China and northern Indochina and, to a lesser extent, Java, which is consistent with the sedimentary chronology of the site. It can be assigned to the "*Stegodon-Ailuropoda* faunal complex" [25–28]. We note the absence of Neogene taxa that persist in the Early Pleistocene and that of two key-species, *Pachycrocuta brevirostris* and *Gigantopithecus blacki*, which are good indicators of pre-300 kyr faunas in the region [29–31]. The archaic *Stegodon* persisted in Asia most likely until the end of the Late Pleistocene [32]. We recovered herbivores including *Tapirus*, *Stegodon,* and Rhinocerotidae, animals that were adapted to canopied woodlands in the area. We also found animals such as the *Bos* species, small-sized Caprinae and large-sized Cervidae (possibly *Rusa unicolor*), which are all known to exhibit a great variability in their preferred habitats, from closed and intermediate forests to open grassland [33], and feeding behaviour.

Ancient proteins analyses

The enamel from the TNH2-1 tooth specimen was analysed using nanoLC-MS/MS and the recently developed approach for ancient enamel proteomes [29]. The TNH2-1 proteome is composed of a common set of enamel-specific proteins, all of which have previously been observed in Pleistocene enamel proteomes [34-36] (Table S6). The enamel proteome has elevated levels of diagenetic protein modifications (Fig. S4A-D, Table S7) and preserves serine (S) phosphorylation within the S-x-E motif previously observed in ancient dental enamel [34,35] (Fig. S4E). Based on proteome composition and modification, as well as the absence of peptides matching to any of these proteins in our extraction and mass spectrometry blanks, we consider our proteomic data as indicative of endogenous proteins deriving from the sampled enamel.

Unfortunately, no high-confidence peptides overlapped diagnostic amino acid positions with sequence differences between *H. sapiens*, Denisovans, or Neanderthals, making further taxonomic assignment based on palaeoproteomics impossible. This is in line with previous research, which indicated that closely related hominin populations can be distinguished based on dentine and bone proteomes, while enamel proteomes are less informative in the context of close phylogenetic proximity [35]. Nevertheless, by comparing the sequences recovered from the TNH2-

1 enamel proteome with that of extant hominids for which protein sequences are available, we find that the specimen belongs to a member of the genus *Homo* (Table S8).

The absence of peptides specific to male-diagnostic amelogenin Y (AMELY) suggests that either the sampled molar was from a female individual or that AMELY-specific peptides were not observed due to degradation beyond the limit of detection of the instrument.

External and internal structural analyses of the tooth

Externally, the TNH2-1 crown displays a coarse wrinkling pattern that is found in Pleistocene *Homo* (*H. erectus* s.l., European and Asian Middle Pleistocene *Homo* and Neanderthals), but is rare in modern *H. sapiens*. The mid-trigonid crest is well developed as commonly recorded in European Middle Pleistocene *Homo* and Neanderthals, while it is generally absent or less frequent in *H. erectus* s.l. and fossil and extant *H. sapiens* [37]. Below the external surface, the enamel-dentine junction (EDJ) of the tooth shows the dentine horns of the five main cusps and of a tuberculum intermedium and a low but uninterrupted mid-trigonid crest (Fig. 2A-H, Fig. S2; Supplementary Material). The latter feature is generally found in Neanderthals (80-100% depending on the molar position) [38-40] but is less frequent in *H. erectus* s.l. and *H. sapiens* [41–47] (Fig. S5). In addition, the EDJ of TNH2-1 shows an internally-positioned metaconid reminiscent of Neanderthal molars [40] and a low crown topography similar to that of *H. erectus* [41–47]. These features, as well as a slight buccal shelf present on the EDJ of TNH2-1, are all expressed on the EDJ of the Denisovan molars from Baishiya Karst Cave (Xiahe, Gansu, China) (Fig. S5) [15]. TNH2-1 dentine differs from the much higher and proportionally more mesiodistally compressed EDJ of Neanderthals and *H. sapiens* [39,40], as well as from the shorter dentine horns and more densely wrinkled occlusal basin of *H. erectus* s.l. [41–47] (Fig. S5).

In terms of absolute dimensions, only Asian Middle Pleistocene *Homo* have larger tooth crowns than TNH2-1 (Tables S9, S10). TNH2-1 crown metrics are within the ranges of variation for *H. erectus* s.l., *H. antecessor*, Asian Middle Pleistocene *Homo* and Neanderthals, but they statistically differ from the smaller crowns of European Middle Pleistocene *Homo* and from Pleistocene and Holocene *H. sapiens* (Fig. 2I-J; Tables S10, S11). With respect to tooth crown tissue proportions, TNH2-1 has a high percentage of crown dentine (Vcdp/Vc: 55.37%) with moderately thick enamel as shown by absolute and relative enamel thickness values (3D AET: 1.18 mm; 3D RET: 17.00; Table S12). These crown tissue proportions match to those of the

nearly unworn M2 of the Xiahe mandible [15] (Vcdp/Vc: 54.62%; 3D AET: 1.47 mm; 3D RET: 18.97) and the upper molar of Denisova 4 (3D RET: 15.27; B. Viola, pers. comm.), but within the ranges of variation of all comparative fossil and extant human groups (Fig. S6A-C; Tables S12, S13). Three-dimensional maps of topographic enamel thickness distribution show that TNH2-1 has the thickest enamel at the top of the hypoconid and hypoconulid cusps and in the distobuccal quarter of the crown (Fig. S6D). In comparison, all other samples tend to have the thickest enamel distributed on all buccal cusps and more spread on the buccal aspect of the crown, even if variable between groups and between molar positions. The M2 of the Xiahe specimen shows thicker enamel spread along the buccal crown aspect but its distribution pattern is partly obliterated by occlusal wear.

The EDJ shape of TNH2-1 was quantitatively compared with those of Pleistocene and Holocene human groups using geometric morphometrics (Supplementary materials). Landmark-based and surface deformation-based approaches were used, with both methods similarly distinguishing between *H. erectus* s.l., European Middle Pleistocene *Homo* and Neanderthals and *H. sapiens* using canonical variate and a between-group principal component analyses (Fig. 3, Fig. S7). Along CV2 and bgPC1, the higher EDJ and more externally set dentine horns of Neanderthals and *H. sapiens* are discriminated from the lower and more centrally positioned dentine horns of *H. erectus* molars. The CV1 and bgPC2 axes separate Neanderthals from modern humans, with the former having more internally placed mesial dentine horns and a more developed hypoconulid than the latter. TNH2-1 falls outside the ranges of all other groups. It has an intermediate EDJ shape between the low crown of *H. erectus* (but exceeding the variation of the latter group along CV1 and bgPC2) and the cusp position of Neanderthal molars (even if outside their range of variation along CV2 and bgPC1). TNH2-1's closest morphological affinity lies with the Denisovan specimen Xiahe, which also displays Neanderthal-like features (Fig. 3, Fig. S7).

Discussion

Reconstructing dispersals and ultimately evolutionary trajectories of *Homo* in Asia depends on a currently poor fossil record. The Asian late Middle Pleistocene fossil record is mostly limited to the eastern part of the continent [4,8–10,15,48]. Any additional human remains from this time period documenting the evolution of *Homo* in southern Asia might thus help confirm previous

hypotheses or reveal new lineages. Proteomic analysis of the TNH2-1 molar indicates that it belongs to a female individual of the genus *Homo*. Morphometric analyses of the external and internal crown structural organisation allow us to reject a number of hypotheses regarding species assignment. TNH2-1 has large crown dimensions and a complex occlusal surface that differentiates it from the smaller and morphologically simpler teeth of *H. floresiensis* [49], *H. luzonensis* [50] and *H. sapiens*. The EDJ shape shows a mixture of Neanderthal-like and *H. erectus*-like features, closely resembling the M1 morphology of the Denisovan specimen from Xiahe (Fig. 2, Fig. S5). The similarities between TNH2-1 and *H. erectus* are mostly related to the proportionally lower crown, although *H. erectus* molars display even lower molar crowns and a narrower occlusal basin (Fig. 2, Fig. S5). The Lao fossil shows clear Neanderthal-like features such as a well-developed mid-trigonid crest and internally-positioned mesial dentine horns, but differs with its much lower EDJ topography and occlusal basin shape.

The differences from Neanderthals that we observe do not preclude TNH2-1 from belonging to this taxon and would make it the south-eastern-most Neanderthal fossil ever discovered. However, considering the morphological particularities of TNH2-1 in unison, as well as the high-degree of morphodimensional similarities with the molars of the Denisovan specimen from Xiahe, the most parsimonious hypothesis is that TNH2-1 belongs to this sister group of Neanderthals. If TNH2-1 indeed belongs to a Denisovan, this occurrence, along with the recent discovery of a Denisovan mandible from the Tibetan Plateau, a high-altitude, hypoxic environment [15], would suggest that this Pleistocene Asian population possessed a high degree of plasticity to adapt to very diverse environments [51]. Available Denisovan dental remains indicate a mixture of traits consistent with the current paleogenetic evidence that Denisovans and Neanderthals are sister taxa [13,14,51–53] and are therefore expected to share some craniodental features [15,54]. This is further supported by recent analyses that identified possible Denisovan skeletal characteristics based on unidirectional methylation changes including traits that have been linked to Chinese fossils such as Xujiayao and Xuchang [9,54]. Denisovans are notable for their large dentition, with some Neanderthal-like crown features [15,48,54] , as well as distinctive cusp and root morphology [14–16]. In the absence of molecular analyses, looking for these combined features in the Asian human fossil record, including in fossils like the Penghu 1 mandible from the Taiwan Strait [55], may help identify more Denisovan specimens (Fig. S8).

The alternative hypothesis that TNH2-1 belongs to a group of Neanderthals that made an incursion into southeast Asia (see for example discussions on fossils that may demonstrate this dispersal from Maba and Dali)[56, 57] cannot be outright rejected.

The tooth from Tam Ngu Hao 2 Cave in Laos thus provides direct evidence of a Denisovan or Neanderthal female individual with associated fauna in mainland Southeast Asia by 164-131 kyr. This discovery further attests that this region was a hotspot of diversity for the genus *Homo* (Fig. S8), with the presence of at least five late Middle to Late Pleistocene species: *H. erectus* [58], Denisovans/Neanderthals, *H. floresiensis* [49], *H. luzonensis* [50] and *H. sapiens* [20–22].

Data and material availability: All mass spectrometry proteomics data have been deposited in the ProteomeXchange Consortium (http://proteomecentral.proteomexchange.org) via the PRIDE partner repository with the dataset identifier PXD018721.

References

1. Baab, K. L. in *Handbook of Paleoanthropology 2.* (eds. Henke, W. & Tattersall, I.) 2189–2219 (Springer, 2015).

2. Kaifu, Y. *et al.* Taxonomic affinities and evolutionary history of the Early Pleistocene hominids of Java: dentognathic evidence. *Am. J. Phys. Anthropol.* **128(4)**, 709-726 (2005).

3. Schwartz, J. H. & Tattersall, I. *The Human Fossil Record: Craniodental Morphology of Genus Homo (Africa and Asia), Vol. 2*. (Wiley-Liss, Inc., 2003).

4. Athreya, S. & Wu, X. A multivariate assessment of the Dali hominin cranium from China: Morphological affinities and implications for Pleistocene evolution in East Asia. *Am. J. Phys. Anthropol.* **164(4)**, 679-701 (2017).

5. Bae, C.J. The late Middle Pleistocene hominin fossil record of eastern Asia: Synthesis and review. *Am J. Phys. Anthropol* **143**, 75-93 (2010).

6. Xing, S., Martinón-Torres, M., Bermúdez de Castro, J.M., Wu, X. & Liu, W. Hominin

teeth from the early Late Pleistocene site of Xujiayao, Northern China. *Am J. Phys. Anthropol.* **156**, 224-240 (2015).

7. Roksandic, M., Radović, P., Wu, X.-J. & Bae, C.J. Resolving the 'muddle in the middle': The case for *Homobodoensis* sp. nov. *Evol. Anthropol*. (2021). doi:10.1002/evan.21929.

8. Ji, Q., Wu, W., Ji, Y., Li, Q. & Ni, X. Late Middle Pleistocene Harbin cranium represents a new *Homo* species. *Innov.* **2**, 100132 (2021).

9. Li, Z.-Y. *et al.* Late Pleistocene archaic human crania from Xuchang, China. *Science* **355**, 969–972 (2017).

10. Wu, X. J. *et al.* Archaic human remains from Hualongdong, China, and Middle Pleistocene human continuity and variation. *Proc. Natl. Acad. Sci. U. S. A.* **116**, 9820–9824 (2019).

11. Stringer, C. The status of *Homo heidelbergensis* (Schoetensack 1908). *Evol. Anthropol.* **21**, 101–107 (2012).

12. Liu, W., Wu, X.J., Xing, S. & Zhang, Y.Y. Human Fossils in China (Science Press, 2014).

13. Krause, J. *et al.* The complete mitochondrial DNA genome of an unknown hominin from southern Siberia. *Nature* **464**, 894–897 (2010).

14. Sawyer, S. *et al.* Nuclear and mitochondrial DNA sequences from two Denisovan individuals. *Proc. Natl. Acad. Sci. U. S. A.* **112**, 15696–15700 (2015).

15 Chen, F. *et al.* A late Middle Pleistocene Denisovan mandible from the Tibetan Plateau. *Nature* **569**, 409–412 (2019).

16. Slon, V. *et al.* A fourth Denisovan individual. *Sci. Adv.* **3**, e1700186 (2017).

17. Jacobs, Z. *et al.* Timing of archaic hominin occupation of Denisova Cave in southern Siberia. *Nature* **565**, 594–599 (2019).

18. Teixeira, J. C. *et al.* Widespread Denisovan ancestry in island Southeast Asia but no evidence of substantial super-archaic hominin admixture. *Nat. Ecol. Evol.* **5**, 616-624 (2021).

19. Larena, M. *et al.* Philippine Ayta possess the highest level of Denisovan ancestry in the world. *Curr. Biol.* **31(19)**, 4219-4230 (2021).

20. Demeter, F. *et al.* Anatomically modern human in Southeast Asia (Laos) by 46 ka. *Proc. Natl. Acad. Sci. U. S. A.* **109**, 14375–14380 (2012).

21. Demeter, F. *et al.* Early modern humans and morphological variation in Southeast Asia: Fossil evidence from Tam Pa Ling, Laos. *PLoS One* **10(4)**, e0121193.

22. Shackelford, L. *et al.* Additional evidence for early modern human morphological diversity in Southeast Asia at Tam Pa Ling, Laos. *Quat. Int.* **466**, 93–106 (2018).

23. Al Qahtani, S. J. & Liversidge, H. M. The London atlas of human tooth development and eruption. *Am. J. Phys. Anthropol.* **142**, 481–490 (2010).

24. Bacon, A. M. *et al.* Late Pleistocene mammalian assemblages of Southeast Asia: New dating, mortality profiles and evolution of the predator-prey relationships in an environmental context. *Palaeogeogr. Palaeoclimatol. Palaeoecol.* **422**, 101–127 (2015).

25. Colbert, E. H. & Hooijer, D. A. Pleistocene Mammals From the Limestone Fissures of Szechwan, China. *Bull. Amer. Mus. Nat. Hist* **102** (1953).

26. Wang, W. *et al.* Sequence of mammalian fossils, including hominoid teeth, from the Bubing Basin caves, South China. *J. Hum. Evol.* **52**, 370–379 (2007).

27. Rink, W. J., Wei, W., Bekken, D. & Jones, H. L. Geochronology of Ailuropoda-Stegodon fauna and *Gigantopithecus* in Guangxi Province, southern China. *Quat. Res.* **69**, 377–387 (2008).

28. Bacon, A.-M. *et al.* Nam Lot (MIS 5) and Duoi U'Oi (MIS 4) Southeast Asian sites revisited: Zooarchaeological and isotopic evidence. *Palaeogeogr. Palaeoclimatol.*

Palaeoecol. **512**, 132–144 (2018).

29. Ciochon, R. *et al.* Dated co-occurrence of *Homo erectus* and *Gigantopithecus* from Tham Khuyen Cave, Vietnam. *Proc. Natl. Acad. Sci. U. S. A.* **93**, 3016–3020 (1996).

30. Zhang, Y. *et al.* New 400-320ka *Gigantopithecus blacki* remains from Hejiang Cave, Chongzuo City, Guangxi, South China. *Quat. Int.* **342**, 35–45 (2014).

31. Bocherens, H. *et al.* Flexibility of diet and habitat in Pleistocene South Asian mammals: Implications for the fate of the giant fossil ape *Gigantopithecus*. *Quat. Int.* **434A**, 148–155 (2017).

32. Turvey, S.T., Tong, H., Stuart, A.J. & Lister, A.M. Holocene survival of Late Pleistocene megafauna in China: A critical review of the evidence. *Quat. Sci. Rev*. **76**, 156-166 (2013).

33. Bacon, A.M. et al. A multi-proxy approach to exploring *Homo sapiens*' arrival, environments and adaptations in Southeast Asia. *Sci Rep*. **11**, 1-14 (2021).

34. Cappellini, E. *et al.* Early Pleistocene enamel proteome from Dmanisi resolves *Stephanorhinus* phylogeny. *Nature* **574**, 103–107 (2019).

35. Welker, F. *et al.* The dental proteome of *Homo antecessor*. *Nature* **580**, 235-238 (2020).

36. Welker, F. *et al.* Enamel proteome shows that *Gigantopithecus* was an early diverging pongine. *Nature* **576**, 262-265 (2019).

37. Bailey, S. E. & Hublin, J.-J. in *Anthropological Perspectives on Tooth Morphology* (eds. Scott, G. R. & Irish, J. D.) 222–249 (Cambridge University Press, 2013).

38. Bailey, S. E., Skinner, M. M. & Hublin, J. J. What lies beneath? An evaluation of lower molar trigonid crest patterns based on both dentine and enamel expression. *Am. J. Phys. Anthropol.* **145**, 505–518 (2011).

39. Skinner, M. M. *et al.* A dental perspective on the taxonomic affinity of the Balanica

mandible (BH-1). *J. Hum. Evol.* **93**, 63–81 (2016).

40. Olejniczak, A. J. *et al.* Morphology of the enamel-dentine junction in sections of anthropoid primate maxillary molars. *J. Hum. Evol.* **53(3)**, 292-301 (2007).

41. Zanolli, C. Molar crown inner structural organization in Javanese *Homo erectus*. *Am. J. Phys. Anthropol.* **156**, 148–157 (2015).

42. Zanolli, C. *et al.* Evidence for increased hominid diversity in the Early to Middle Pleistocene of Indonesia. *Nat. Ecol. Evol.* **3**, 755–764 (2019).

43. Zanolli, C. *et al.* The late Early Pleistocene human dental remains from Uadi Aalad and Mulhuli-Amo (Buia), Eritrean Danakil: Macromorphology and microstructure. *J. Hum. Evol.* **74**, 96–113 (2014).

44. Zanolli, C. & Mazurier, A. Endostructural characterization of the *H. heidelbergensis* dental remains from the early Middle Pleistocene site of Tighenif, Algeria. *Comptes Rendus Palevol* **12(5)**, 293-304 (2013)

45. Xing, S., Martinón-Torres, M. & Bermúdez De Castro, J. M. The fossil teeth of the Peking Man. *Sci. Rep.* **8**, 2066 (2018).

46. Xing, S. *et al.* Hominin teeth from the Middle Pleistocene site of Yiyuan, Eastern China. *J. Hum. Evol.* **95**, 33–54 (2016).

47. Xing, S. *et al.* Middle Pleistocene hominin teeth from Longtan Cave, Hexian, China. *PLoS One* **9**, 1–38 (2014).

48. Pan, L., Dumoncel, J., Mazurier, A. & Zanolli, C. Hominin diversity in East Asia during the Middle Pleistocene: A premolar endostructural perspective. *J. Hum. Evol.* **148**, 102888 (2020).

49. Morwood, M. J. *et al.* Further evidence for small-bodied hominins from the Late Pleistocene of Flores, Indonesia. *Nature* **437**, 1012-1017 (2005).

50. Détroit, F. *et al.* A new species of *Homo* from the Late Pleistocene of the Philippines. *Nature* **568**, 181–186 (2019).

51. Jacobs, G. S. *et al.* Multiple Deeply Divergent Denisovan Ancestries in Papuans. *Cell* **177**, 1010-1021.e32 (2019).

52. Slon, V. *et al.* The genome of the offspring of a Neanderthal mother and a Denisovan father. *Nature* **561**, 113–116 (2018).

53. Browning, S. R., Browning, B. L., Zhou, Y., Tucci, S. & Akey, J. M. Analysis of human sequence data reveals two pulses of archaic Denisovan admixture. *Cell* **173**, 53-61.e9 (2018).

54. Gokhman, D. *et al.* Reconstructing Denisovan anatomy using DNA methylation maps. *Cell* **179**, 180-192.e10 (2019).

55. Chang, C. H. *et al.* The first archaic *Homo* from Taiwan. *Nat. Commun.* **6**, 1–33 (2015).

56. Wu, X. & Poirier, F.E. *Human Evolution in China. A metric description of the fossils and a review of the sites*. (Oxford University Press, 1995).

57. Xiao, D. et al. Metric and geometric morphometric analysis of new hominin fossils from Maba (Guangdong, China). *J. Hum. Evol*. **74**, 1-20 (2014).

58. Rizal, Y. *et al.* Last appearance of *Homo erectus* at Ngandong, Java, 117,000–108,000 years ago. *Nature* **577**, 381-385 (2020).

Acknowledgements: We thank the Ministry of Information, Culture and Tourism of Lao PDR for encouraging and supporting our work, marking almost 20 years of collaboration. We thank the authorities of Xon district, Hua Pan Province and the villagers of Long Gua Pa village for their continuous support of our numerous years of fieldwork. We also thank many curators and colleagues who granted access to the comparative fossil and recent hominin specimens for scanning, as well as the online sharing platforms of the Nespos society (http://www.nespos.org) and ESRF Paleontological database (http://paleo.esrf.eu). We acknowledge A. Mazurier and R. Macchiarelli (University of Poitiers), A. Bravin, C. Nemoz and P. Tafforeau (ESRF Synchrotron), P. Bayle and F. Santos (University of Bordeaux), O. Kullmer and F. Schrenk (Senckenberg Museum), F. Bernardini and C. Tuniz (ICTP Trieste), J. Braga and J. Dumoncel (University of Toulouse) for analytical support, microtomographic scanning and sharing of material. We gratefully acknowledge support from the CNRS/IN2P3 Computing Center (Lyon - France) for providing computing and data-processing resources needed for this work. Our thanks also go to Christine Lefèvre, Joséphine Lesur and Aurélie Verguin (Laboratoire Mammifères et Oiseaux, Anatomie comparée, MNHN, Paris) for access to comparative mammalian collections. Warm thanks to Jeremy Kazan (Taxidermie, MNHN, Paris) for having, as usual, wonderfully casted and reproduced the specimen. M.W.M. thanks George Morgan and Mark Keene at Adelaide Petrographics for expertly making the micromorphology thin sections.

Funding:
Australian Research Council (ARC) Future Fellowship award (FT180100309) (MWM)
Australian Research Council (ARC) Discovery grant (DP170101597) (KEW)
Marie Skłodowska Curie Individual Fellowship (no. 795569) (FW)
Marie Skłodowska-Curie European Training Network (ETN) TEMPERA, a project funded by the European Union's Framework Program for Research and Innovation Horizon 2020 (no. 722606) (EC, JVO, PR)
European Research Council (ERC) under the European Union's Horizon 2020 research and innovation programme (no. 948365) (FW)
VILLUM FONDEN (no. 17649) (EC)
European Union's Framework Program for Research and Innovation Horizon 2020 (no. 819960) (MMS)
Novo Nordisk Foundation (grant number NNF14CC0001)
National Geographic Society (NGS-399R-18) (LS)
MNHN/University Paris Diderot/Sorbonne Paris Cité, France
CNRS/Université de Paris; Université de Strasbourg, France
Department of Human Evolution, Max Planck Institute for Evolutionary Anthropology, Leipzig, Germany
Sodipram company, France

Author Contributions:
Conceptualization: FD, LS, AMB, TS, VS, TL

Methodology: CZ, MMS, KEW, RJ, RMB

Formal analysis: CZ, MMS, AMB, POA, MWM, LP, XS, J-JH, PD, J-LP, QB, FW, PLR, JVO, EC, HMC, KEW, RJ, J-XZ, RMB

Investigation: FD, CZ, LS, PD, J-LP, ES, SF, TD, QB, AMB, FW, PLR, JVO, EC, HMC, KEW, RJ, J-XZ, RMB

Writing – original draft: FD, CZ, LS

Writing – review & editing: EW, J-JH, FW, PD, POA, MWM, KW

Supervision: FD, LS, AMB

Project administration: FD, LS, AMB

Funding acquisition: FD, LS, AMB, KEW, RJ, EC, FW, J-JH, EW

Competing interests: The authors declare no competing interests.

Supplementary Materials

Materials and Methods

Supplementary Text

Figs. S1 to S15

Tables S1 to S17

Data File 1

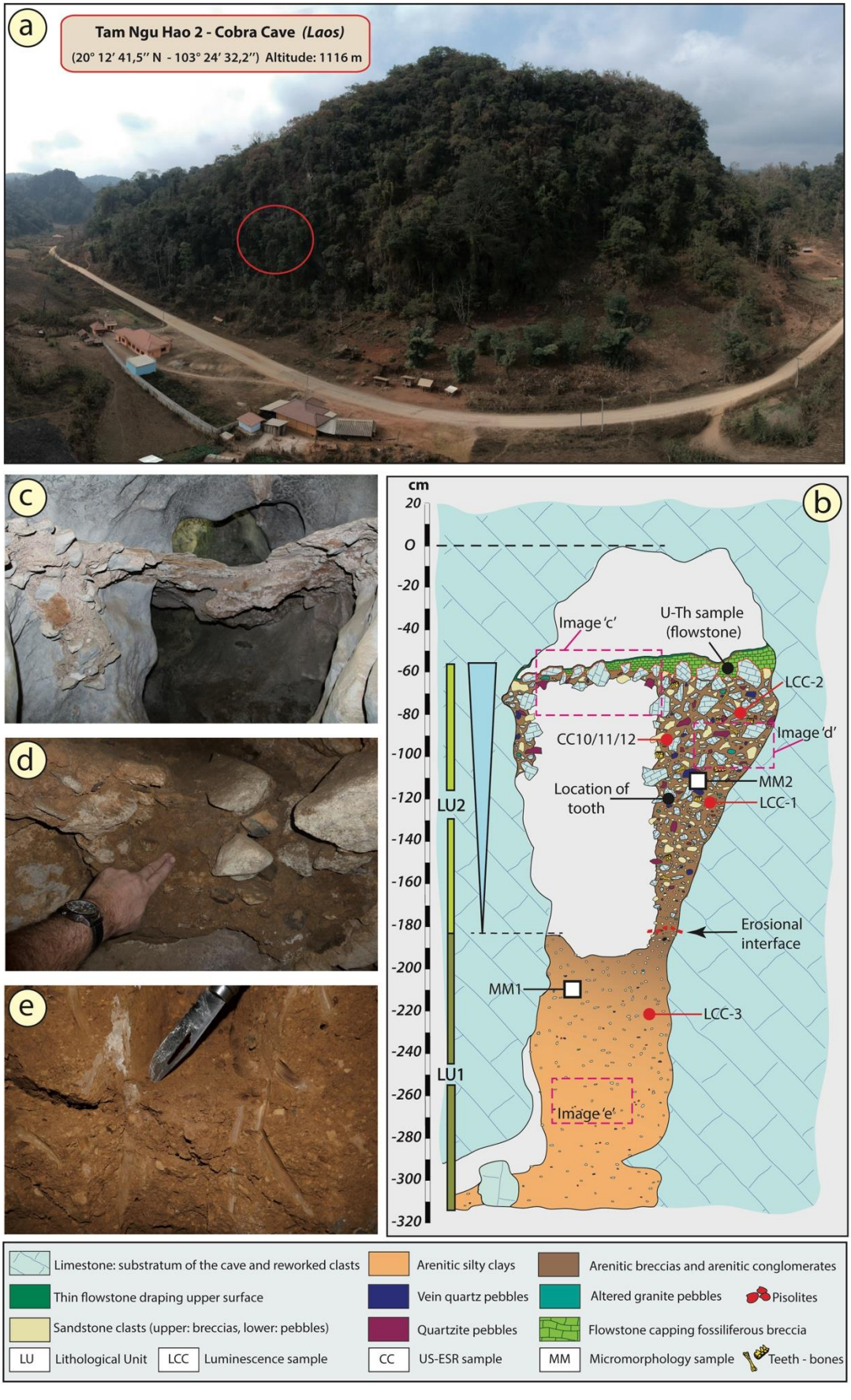
a
Tam Ngu Hao 2 - Cobra Cave (Laos)
(20° 12′ 41,5″ N - 103° 24′ 32,2″) Altitude: 1116 m
c
d
e
b
cm
20
0
-20
-40
-60
-80
-100
-120
-140
-160
-180
-200
-220
-240
-260
-280
-300
-320
LU2
LU1
Image 'c'
U-Th sample (flowstone)
LCC-2
CC10/11/12
Image 'd'
MM2
Location of tooth
LCC-1
Erosional interface
MM1
LCC-3
Image 'e'
Limestone: substratum of the cave and reworked clasts
Thin flowstone draping upper surface
Sandstone clasts (upper: breccias, lower: pebbles)
LU Lithological Unit
LCC Luminescence sample
Arenitic silty clays
Vein quartz pebbles
Quartzite pebbles
CC US-ESR sample
Arenitic breccias and arenitic conglomerates
Altered granite pebbles
Pisolites
Flowstone capping fossiliferous breccia
MM Micromorphology sample
Teeth - bones

514

Fig. 1. Geomorphological context and stratigraphy of TNH2. A) aerial view of the site. The red circle indicates the entrance of Tam Ngu Hao 2 cave; B) stratigraphy and sampling locations of the infilling of the cave, showing Lithological Unit 1 and 2 (LU1 and LU2) with the erosional interface between these layers indicated by a dashed red line; Micromorphological (microstratigraphic) samples (MM1 and MM2) are also shown. Encircled numbers denote approximate positions of photographs in C, D & E; C) view of the flowstone capping the upper remaining part of LU2. D) detail of the arenitic breccia/conglomerate of LU2 ; E) detail of the arenitic silty clay of LU1.

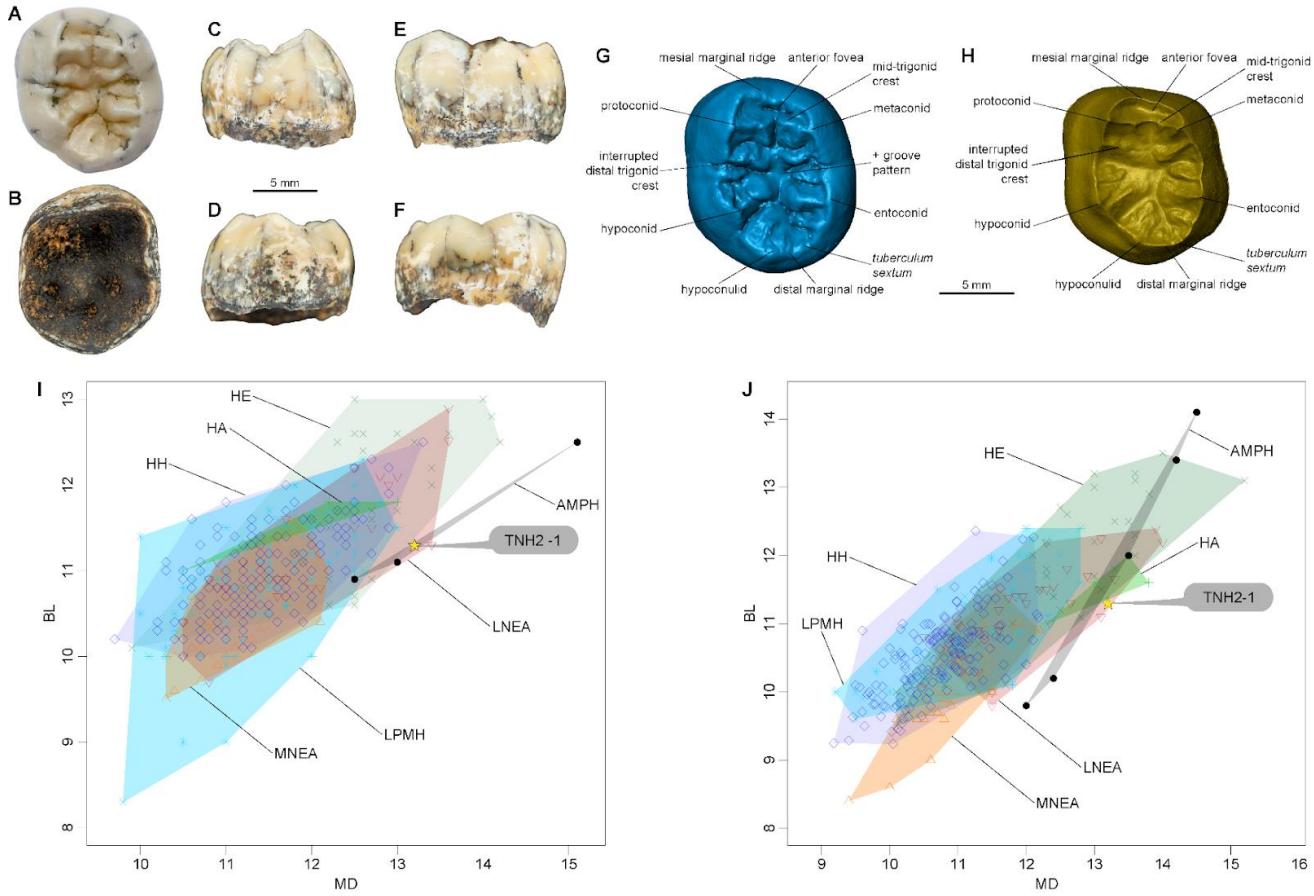

Fig. 2. Morphological and metrical features of the TNH2-1 specimen. A-F, pictures of TNH2 in occlusal (A), inferior (B), mesial (C), distal (D), buccal (E) and lingual (F) views. G-H, virtual renderings of the outer enamel surface (G) and enamel-dentine junction (H) in occlusal view showing the main morphological features. I-J, bivariate scatter plots of the mesiodistal and buccolingual crown dimensions of TNH2 compared with the M1s (I) and M2s (J) of *H. erectus* (HE), *H. antecessor* (HA), Middle Pleistocene Neanderthals (MNEA), Late Pleistocene Neanderthals (LNEA), Asian Middle Pleistocene *Homo* (AMPH), Late Pleistocene modern humans (LPMH) and Holocene humans (HH).

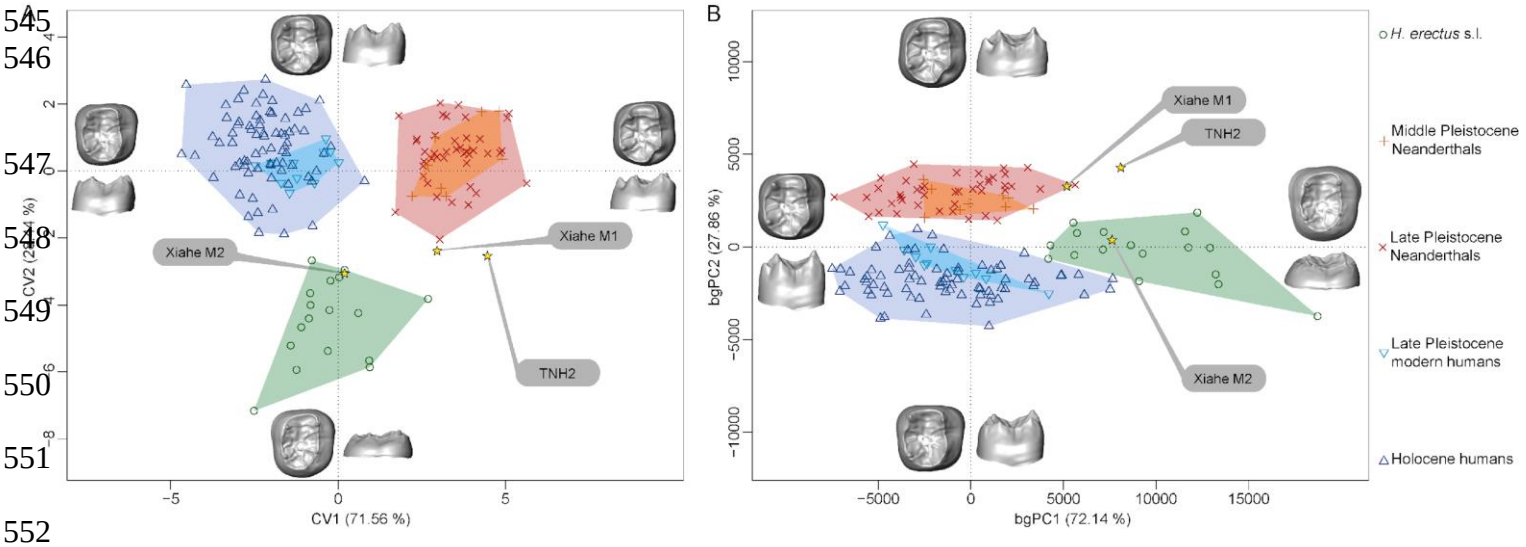

Fig. 3. Canonical variate analysis (A) and between-group principal component analysis (B) of the EDJ deformation-based shape comparison of TNH2-1, *H. erectus* s.l., the Denisovan specimen from Xiahe, Neanderthals and *H. sapiens*.